PHYSICAL REVIEW B **81**, 201401(R) (2010)

In situ observations of self-repairing single-walled carbon nanotubes

Felix Börrnert,[1,*] Sandeep Gorantla,[1] Alicja Bachmatiuk,[1] Jamie H. Warner,[2] Imad Ibrahim,[1,3] Jürgen Thomas,[1] Thomas Gemming,[1] Jürgen Eckert,[1,3] Gianaurelio Cuniberti,[3] Bernd Büchner,[1] and Mark H. Rümmeli[1,3]
[1]*Leibniz-Institut für Festkörper- und Werkstoffforschung Dresden e.V., Postfach 27 01 16, 01171 Dresden, Germany*
[2]*Department of Materials, University of Oxford, Parks Road, Oxford OX1 3PH, United Kingdom*
[3]*Technische Universität Dresden, 01062 Dresden, Germany*
(Received 18 March 2010; published 5 May 2010)

Single-walled carbon nanotubes are shown to have self-repairing capabilities exceeding that predicted by theory. Time-series aberration-corrected low-voltage transmission electron microscopy is used to study the defect dynamics of single-walled carbon nanotubes *in situ*. We confirm experimentally previous theoretical predictions for the agglomeration of adatoms forming protrusions and subsequent ejection. An explanation for the preferred destruction of smaller-diameter tubes is proposed. The complete healing of a ~20-atom multivacancy in a nanotube wall is shown while theory only predicts the healing of much smaller holes.

DOI: 10.1103/PhysRevB.81.201401 PACS number(s): 61.48.De, 82.37.−j

Single-walled carbon nanotubes (SWNTs) are well-recognized potential building blocks for future nanodevices.[1] Defects in ordered systems can destroy or introduce features attractive for applications so they are the object of vivid research.[2,3] The defect structure and dynamics of SWNTs is much discussed throughout the literature, mostly from the theoretical side because of a lack of suitable experimental techniques to adequately engage this problem.[4–12] The mechanism on how carbon nanotubes retain their general structure under irradiation is usually described in terms of material loss and subsequent surface reconstruction.[5,10] For example, carbon atoms can migrate along the tube wall to provide construction material.[12,13] Small vacancy clusters can be closed through Stone-Wales-type transformations.[8] However, calculations suggest the formation of big holes is unfavorable as compared to multiple small vacancies and that network reconstruction is more efficient in small-diameter nanotubes.[7] Recent advances in transmission electron microscopy have allowed the direct imaging of nanostructures at the atomic scale.[14,15] However, network reconstruction in nanotubes has only been observed in large-diameter multiwalled carbon nanotubes through the interaction of the different walls.[16,17] We are not aware of any reports for SWNTs.

Time series of aberration-corrected low-voltage high-resolution transmission electron microscopy (TEM) is a valuable tool to directly observe the changes in the specimen atomic structure *in situ*. During irradiation with 80 kV electrons, an ideal SWNT should be stable.[18] Nevertheless, defective regions, highly stressed structures, or contaminated sites have a reduced energy barrier for knock-on damage.[19]

In this Rapid Communication, we study self-healing mechanisms in SWNTs using low-voltage high-resolution transmission electron microscopy. The autoejection of carbon material and the closing of 20-atom holes is shown.

The SWNTs employed were produced by a laser ablation route and have a mean diameter of approximately 1.5 nm.[20] They were first annealed in air at 380 °C for 0.5 h. A fraction of the tubes were then filled with [6,6]-phenyl-C_{61}-butyric-acid-methyl-ester (PCBM) (Ref. 21) by annealing them in the presence of PCBM in a sealed quartz ampule with an internal pressure of 10^{-3} Pa at 550 °C for 5 days. For imaging, the sample was drop coated onto standard lacey carbon TEM grids. A FEI Titan^3 80–300 transmission electron microscope with a CEOS aberration corrector for the objective lens, operating at an acceleration voltage of 80 kV, equipped with a Gatan UltraScan 1000 camera was used. All studies were conducted at room temperature. During a time series, an image was taken every 5 s with an acquisition time of 0.5 s and all images were compiled into motion pictures. The contrast of the micrographs was enhanced through Fourier filtering by cutting frequencies beyond the information limit of the microscope. The chirality of the SWNTs was determined by analyzing the Fourier-transformed TEM images and measuring the corrected SWNT diameter.[14] Simulations of the imaging process were obtained using JEMS electron microscopy software.[22] For comparison, noise was added to the simulated images and the same Fourier filtering applied as for the TEM images.

In Fig. 1, frames (a)–(c) show a series of TEM images of a SWNT with defects. The time span between each frame is 5 s. In frame (a), a humplike defect in the wall of the tube is indicated by an arrow. The chirality of the tube was deter-

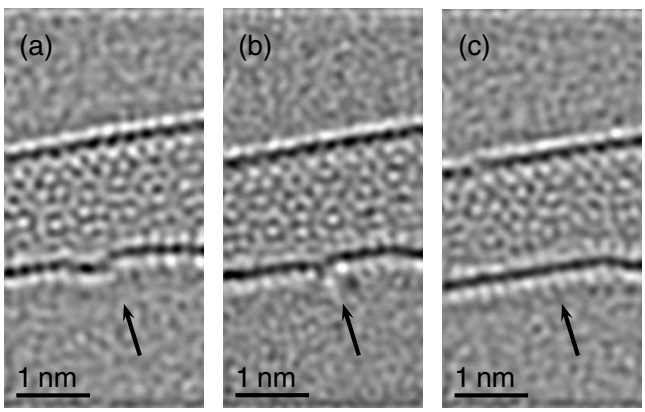

FIG. 1. *In situ* TEM observation of material ejection from a SWNT. (a) Humplike defect in the wall (see arrow), (b) formation of a protrusion, and (c) defect has disappeared. The time elapsed between each frame is 5 s.

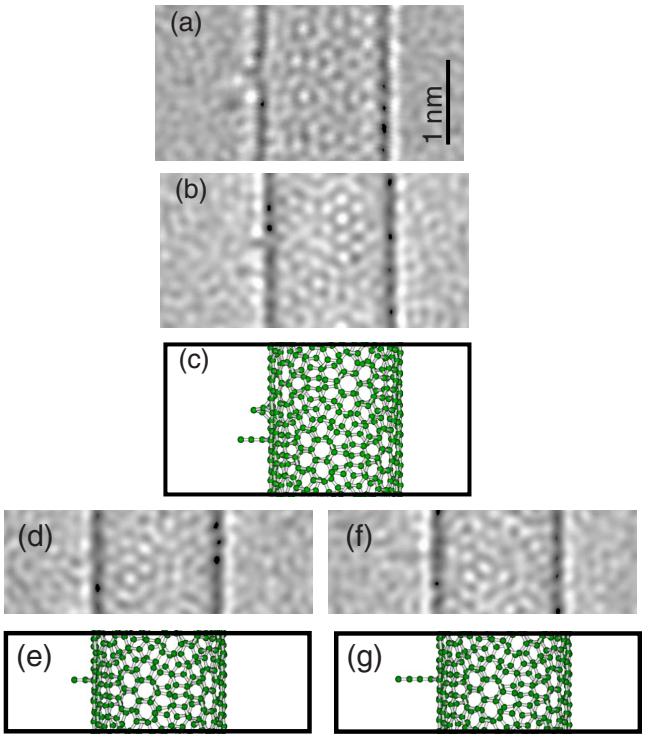

FIG. 2. (Color online) Comparison of original and simulation of a TEM image of the protrusion. (a) Fourier-filtered TEM image [cut from Fig. 1(b)], (b) Fourier-filtered output of a multislice simulation of the imaging process of a (14,9) tube with two three-atom protrusions, and (c) ball-and-stick illustration of the underlying molecular model for the simulation. (d) and (e) Simulation and model of a two-atom protrusion, and (f) and (g) a four-atom protrusion. Simulation parameters: accelerating voltage 80 kV, chromatic aberration 1.1 mm, spherical aberration 0.002 mm, defocus 1.8 nm, energy spread 0.8 eV, defocus spread 6.6 nm, and noise 2%.

mined to be (14, 9) from the Fourier transform of the micrograph as explained by Hashimoto *et al.*[14] Frame (b) features a dark spot outside the wall at the same position. The humplike feature has now shrunk significantly. In frame (c), there is no longer any defect. The dark spot in the micrograph shows material bound to the wall for a nominal time span, viz., the cameras acquisition time. More details of the evolution of the defect can be observed in a motion picture compiled from the image series.[23] Simulations of the imaging process (see Fig. 2) reveal that this protrusion comprises three carbon atoms. The feature beneath the chainlike protrusion can be modeled by a three-atom agglomeration as shown in the ball-and-stick model of Fig. 2(c). We performed various imaging simulations with different configurations of the underlying model that had varying numbers of atoms in the defect. For these simulations, the recording parameters from the original micrographs were used. The simulation study indicates that a protrusion containing less than three atoms cannot be observed in the vicinity of the wall. Protrusions with more than three atoms show a significantly larger footprint than that observed in the micrographs. The formation of three-atom protrusions agrees well with a mechanism proposed by Tsetseris and Pantelides where they studied the stability of self-interstitial structures on graphene and

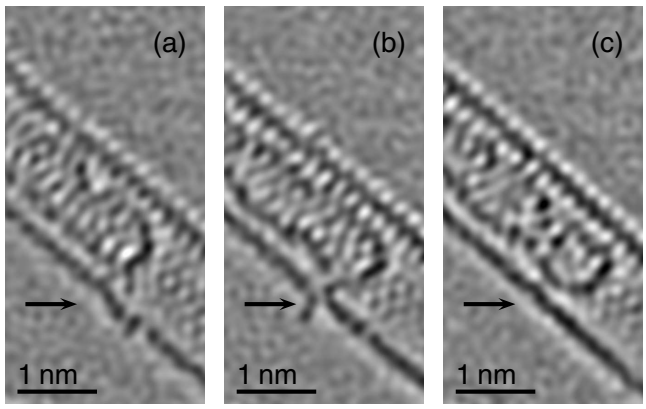

FIG. 3. *In situ* TEM observation of the ejection of material from a SWNT with an inner tube section formed from coalesced PCBM. (a) Material attached to the tip of an inner tube, (b) the material protruding the host wall, and (c) the host wall closed and the material has autoejected. The time elapsed between the frames is 15 s and 10 s, respectively.

SWNTs using first-principles calculations.[12] They show that C agglomeration is energetically favorable and that three-atom complexes heal out to very mobile protrusions. In our image series, the protrusion vanishes in the last frame, leaving a straight wall. Two possible explanations for the protrusions disappearance are conceivable: either the protrusion becomes mobile on the surface and is incorporated into other defects in the wall or it is ejected from the tube. The latter argument is more probable because if the protrusion were mobile, it could not be imaged. Calculations in a previous study of ours show that a carbon chain is not mobile on such a surface.[24] This was due to the weak delocalization of the double bonds in the lattice of the tube. For the present case, this is not valid because a very short protrusion with a free end can change the bond orientation easily. With increasing length, the chain's mobility is likely to decrease. Our findings are in agreement with previous studies in which the ejection of material from the wall of a SWNT to produce an undisturbed lattice has been proposed.[5,10]

In Fig. 3, frames (a)–(c), a series of TEM images of an inner tube residing in a host SWNT is presented. The chirality of the host tube is (14,8). The inner SWNT formed earlier via the coalescence of the PCBM fullerenes. In panel (a), material is attached to the tip of the inner SWNT. This material is seen to interact with the host wall (indicated by the arrow) and the host wall is perturbed during this process. Eventually part of the carbon chain protrudes through the host wall [panel (b)]. This is similar to observations by Koshino *et al.*[25] in which the passage of hydrocarbon chains through SWNT walls are imaged. However, unlike their observations, here we observe the chain to eject from the host SWNT. The host wall appears undisturbed after the ejection process. The opening of the host wall allowing the ejection of the material might be explained by the fact that contaminants lower the beam damage threshold.[19,26] In addition, the autoejection mechanism could be responsible for the removal of reactive species such as the methoxy group from the PCBM. Such groups act like contaminants disturbing the lattice of the tube.

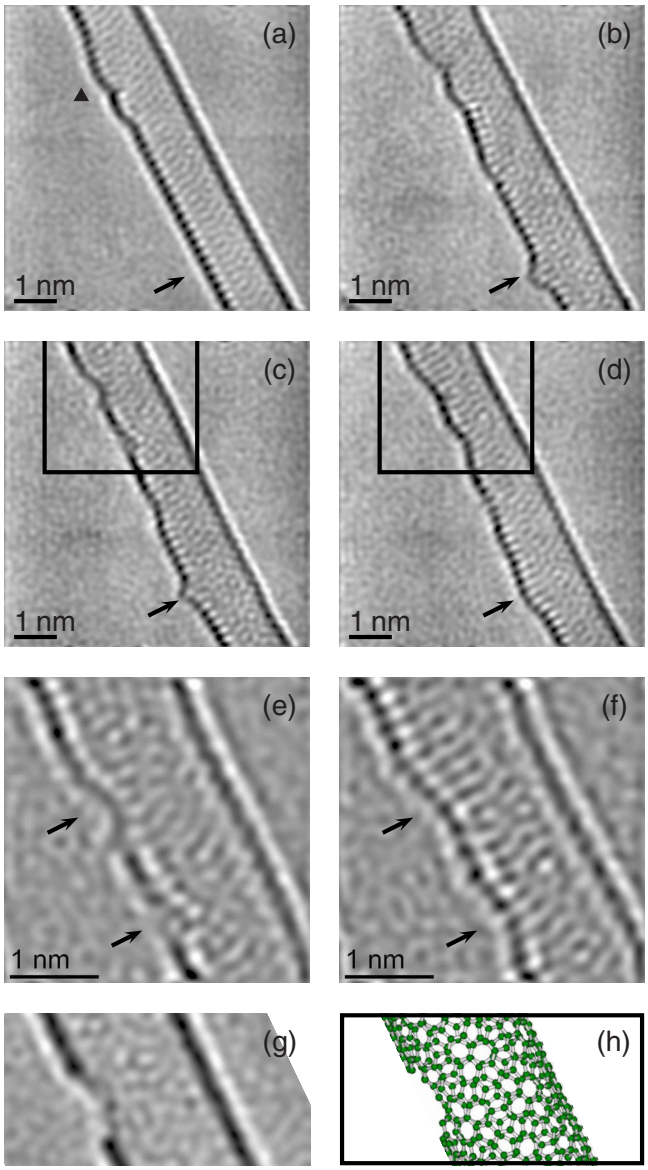

FIG. 4. (Color online) Time series of TEM images showing the defect dynamics of a SWNT. (a) Initial state with a defective region in the upper part (see triangle), (b) emergence of a hump in the lower part, (c) appearance of two holes in the disturbed region and a flattening out of the hump, and (d) reconstruction of the lattice in the upper part. The left wall stays undisturbed. The time elapsed from recording images (a)–(d) is 11.5 min. (e) Magnified section from rectangle in frame (c), region indicated by the box, and (f) magnified section from frame (d). (g) Fourier-filtered output of a multislice simulation of the imaging process of a (13,7) tube with a 21-atom hole, and (h) a ball-and-stick illustration of the underlying molecular model for the simulation. Simulation parameters: accelerating voltage 80 kV, chromatic aberration 1.1 mm, spherical aberration 0.002 mm, defocus 3.5 nm, energy spread 0.8 eV, defocus spread 11 nm, and noise 2%.

Another healing mechanism is demonstrated in Fig. 4. It shows a (13,7) SWNT with a defective region in the left side of the tube [black triangle in frame (a)]. The defective region changes its morphology over the entire time sequence opening up holes and closing again. More details of the evolution of the defects can be observed in a motion picture compiled from the image series.[23] In the lower left part of the tube, the emergence of a hump is depicted as one goes from frame (a) to frame (b)—see arrow. The origin of the additional material for the hump is not clear. Banhart *et al.*[13] found that carbon nanotubes can act as pipes for atom transport. It may be that the removal of material elsewhere in the tube which ejects within the tube provides a source of carbon. In addition, the defects found in the upper left region are continuously reforming and spreading out, e.g., frames (c) and (d). This process could effectively create preferential defect sites further down the tube suitable for the incorporation of carbon. As the notchlike defects spread over a broader region, two holes can be seen to evolve in the upper left region [see frame (e)]. Image simulations allow us to estimate about 20 atoms are missing in the upper hole. Remarkably these holes then close up over a period of 20 s [see panel (f)]. We find no evidence that the holes have rotated or moved elsewhere along the tube. The appearance of new defects in the vicinity of the healing region might be due to the extensive rearrangement of the crystal structure to regain an overall hexagonal lattice. In this case, the electron beam provides the energy for the reconstruction of the sp^2 lattice. Heat might lead to similar processes because it is known from optical spectroscopy studies that annealing CNTs leads to an enhanced crystallinity. The right side of the tube is not affected by the reconstruction processes observed on the left side. Two points of interest may be derived from this fact, first, the morphology changes need an initial defect that lowers the threshold energy for beam damage in agreement with previous observations.[19] Second, the area involved in the reconstruction preferentially spreads along the tube axis. The curvature of the sp^2 lattice seems to prevent the rearrangement of the lattice in this direction. If we assume a unidirectional vibrational potential, the carbon atoms are placed in a planar lattice. A curvature introduced in the lattice lifts this degeneracy and elongates the potential along the tube axis. The vibrational amplitude of the atoms is reduced in the direction of the curvature so that the atoms do not approach each other sufficiently to change binding site. In a previous work, we investigated the impact of electron irradiation at 80 kV accelerating voltage on SWNTs of different diameters.[19] SWNTs with larger diameters of 2.3 nm had defects that were transient and could self-heal while narrower 0.9 nm diameter nanotubes formed defects that led to their destruction. Here we show that the same electron irradiation of tubes with a diameter of 1.4 nm also leads to defects that can self-heal. This supports the hypothesis that the lattice curvature restricts the spreading of the reconstruction region. This effect is more prevalent the narrower the tube. Previous theoretical studies have shown small holes up to six missing atoms can heal in a (10,10) nanotube with a diameter of 1.4 nm in elevated temperatures.[7] Our observations suggest the healing process is capable of sealing significantly larger holes than previously shown and display the need for systematic studies of the maximum ratio of defect size and nanotube diameter.

In this work, we show the autoejection and self-healing dynamics of single-walled carbon nanotubes via aberration-

corrected low-voltage transmission electron microscopy. The agglomeration of atoms forming three-atom protrusions at the nanotube wall is observed, confirming previous theoretical predictions. Moreover, we experimentally demonstrate the complete healing of the tube wall after material ejection. This confirms previous models. An explanation for the preferred destruction of smaller-diameter tubes previously reported is offered. In addition, the closing of multivacancies of up to approximately 20 missing atoms is presented. Hence, single-walled carbon nanotubes have self-repairing capabilities far exceeding that predicted by current theory.

We thank R. Hübel and S. Leger for technical support. S.G. acknowledges the "Pakt für Forschung und Innovation," I.I. the DAAD, and J.E. and M.H.R. the EU (ECEMP) and the Freistaat Sachsen.

*f.boerrnert@ifw-dresden.de

[1] P. Avouris, Acc. Chem. Res. **35**, 1026 (2002).
[2] J.-C. Charlier, Acc. Chem. Res. **35**, 1063 (2002).
[3] C. Gómez-Navarro, P. J. De Pablo, J. Gómez-Herrero, B. Biel, F. J. Garcia-Vidal, A. Rubio, and F. Flores, Nat. Mater. **4**, 534 (2005).
[4] V. H. Crespi, N. G. Chopra, M. L. Cohen, A. Zettl, and S. G. Louie, Phys. Rev. B **54**, 5927 (1996).
[5] P. M. Ajayan, V. Ravikumar, and J.-C. Charlier, Phys. Rev. Lett. **81**, 1437 (1998).
[6] A. V. Krasheninnikov, F. Banhart, J. X. Li, A. S. Foster, and R. M. Nieminen, Phys. Rev. B **72**, 125428 (2005).
[7] J. Kotakoski, A. V. Krasheninnikov, and K. Nordlund, Phys. Rev. B **74**, 245420 (2006).
[8] G.-D. Lee, C. Z. Wang, E. Yoon, N.-M. Hwang, D.-Y. Kim, and K. M. Ho, Phys. Rev. Lett. **95**, 205501 (2005).
[9] A. Tolvanen, J. Kotakoski, A. V. Krasheninnikov, and K. Nordlund, Appl. Phys. Lett. **91**, 173109 (2007).
[10] F. Ding, K. Jiao, Y. Lin, and B. I. Yakobson, Nano Lett. **7**, 681 (2007).
[11] J. Miyawaki, R. Yuge, T. Kawai, M. Yudasaka, and S. Iijima, J. Phys. Chem. C **111**, 1553 (2007).
[12] L. Tsetseris and S. T. Pantelides, Carbon **47**, 901 (2009).
[13] F. Banhart, J. X. Li, and A. V. Krasheninnikov, Phys. Rev. B **71**, 241408(R) (2005).
[14] A. Hashimoto, K. Suenaga, A. Gloter, K. Urita, and S. Iijima, Nature (London) **430**, 870 (2004).
[15] K. Suenaga, H. Wakabayashi, M. Koshino, Y. Sato, K. Urita, and S. Iijima, Nat. Nanotechnol. **2**, 358 (2007).
[16] J. Y. Huang, F. Ding, and B. I. Yakobson, Phys. Rev. B **78**, 155436 (2008).
[17] C. Jin, K. Suenaga, and S. Iijima, Nano Lett. **8**, 1127 (2008).
[18] B. W. Smith and D. E. Luzzi, J. Appl. Phys. **90**, 3509 (2001).
[19] J. H. Warner, F. Schäffel, G. Zhong, M. H. Rümmeli, B. Büchner, J. Robertson, and G. A. D. Briggs, ACS Nano **3**, 1557 (2009).
[20] M. H. Rümmeli, C. Kramberger, M. Löffler, O. Jost, M. Bystrzejewski, A. Grüneis, T. Gemming, W. Pompe, B. Büchner, and T. Pichler, J. Phys. Chem. B **111**, 8234 (2007).
[21] J. C. Hummelen, B. W. Knight, F. LePeq, F. Wudl, J. Yao, and C. L. Wilkins, J. Org. Chem. **60**, 532 (1995).
[22] P. A. Stadelmann, Ultramicroscopy **21**, 131 (1987).
[23] See supplementary material at http://link.aps.org/supplemental/10.1103/PhysRevB.81.201401 for motion pictures compiled from the image series.
[24] F. Börrnert, C. Börrnert, S. Gorantla, X. Liu, A. Bachmatiuk, J.-O. Joswig, F. R. Wagner, F. Schäffel, J. H. Warner, R. Schönfelder, B. Rellinghaus, T. Gemming, J. Thomas, M. Knupfer, B. Büchner, and M. H. Rümmeli, Phys. Rev. B **81**, 085439 (2010).
[25] M. Koshino, N. Solin, T. Tanaka, H. Isobe, and E. Nakamura, Nat. Nanotechnol. **3**, 595 (2008).
[26] T. D. Yuzvinsky, A. M. Fennimore, W. Mickelson, C. Esquivias, and A. Zettl, Appl. Phys. Lett. **86**, 053109 (2005).